

MEDIUM AND LARGE-SCALE VARIATIONS OF DYNAMO-INDUCED ELECTRIC FIELDS FROM AE ION DRIFT MEASUREMENTS

W. R. Coley and J. P. McClure
Center for Space Sciences, Physics Program
The University of Texas at Dallas
Richardson, Texas 75083

Current models of the low latitude electric field are largely based on data from incoherent scatter radars. We are extending these observations through the addition of the rather extensive high quality electric field measurements from the Ion Drift Meter (IDM) aboard the Atmosphere Explorer (AE) spacecraft. We present here some preliminary results obtained from the Unified Abstract files of satellite AE-E. This satellite was active from the end of 1975 through June 1981 in various elliptical and circular orbits having an inclination near 20° . The resulting data can be examined for the variation of ion drift with latitude, longitude, season, solar cycle, altitude, and magnetic activity. The results presented here will deal primarily with latitudinal variations of the drift features.

Figure 1 shows data from a single AE-E orbit. Of particular interest is the upward ion drift enhancement at 2:38 UT. This corresponds to 18:30 solar local time (SLT). This enhancement of the upward drift after sunset prior to reversal is a classic pattern that is often seen both by ground-based radar and satellite. However, on many occasions this prereversal enhancement (PRE) is absent. In order to investigate the reasons for these and other variations of the observed drift features it is of course necessary to deal with large quantities of data.

Figures 2a and 2b show the type of data presentation used in this study. Figure 2a is a "mass plot" of vertical drift data from AE-E obtained from the 15-second average values of the Unified Abstract files. All vertical drifts in the file between -20° and 20° dip latitude (DLAT) for the August-September 1978 time period are plotted versus SLT. In all there are some 6987 points. Figure 2b shows the same data averaged into 30-minute bins. The dotted line represents the 24-hr average vertical drift. For comparison, Figure 3 shows some incoherent scatter radar results from Jicamarca for the July-August 1968-1971 time period (Fejer et al., 1979). In both cases we see the same general features: downward flow at night reversing at 0600 SLT, a daytime peak followed by a decline to a prereversal enhancement between 19 and 20 SLT, and a reversal to downward flow at night.

Figures 4a and 4b cover May-July 1979 from -20° to 20° DLAT. The satellite was in a near-circular orbit during this period within altitudes of 450-475 km. There are some 17,000 points plotted on Figure 4a, most falling in a band some 75 m/s wide. The exception is the large spread in velocity in the post-sunset time period.

The next four figures take the data set of Figure 4 and break it up into 10 degree wide bins of dip latitude. Figures 5 through 8 cover the ranges 10° to 20° DLAT, 0° to 10° DLAT, -10° to 0° DLAT, and -20° to 10° DLAT, respectively. The raw data plots indicate generally a much smaller spread in the vertical ion velocity at any given local time. The averaged plots indicate a systematic variation of the average velocity with latitude. The largest average upward velocity is

found in the most northerly latitude bin (summer hemisphere). The most southerly bin (winter hemisphere) has a net downward velocity. Other features also show latitude dependence; the evening prereversal enhancement is strong in the summer hemisphere and weak or nonexistent in the winter hemisphere.

Figures 9 and 10 show a similar pattern for the Nov 77 ~ Jan 78 time period. Figure 9 shows the 10° to 20° DLAT bin (winter hemisphere). Figure 10 shows the -20° to -10° DLAT bin (summer hemisphere). As before there is a generally upward bias of the drift in the summer hemisphere and a downward bias in the winter hemisphere.

One possible interpretation of this pattern is that the dynamo induced ion velocities are being modified by neutral wind flow, the meridional component of which flows generally from the summer to winter hemisphere under solstice conditions. Dachev and Walker, 1982, calculated the vertical ion drift velocity imposed by dynamo electric fields and the zonal and meridional winds in the 19-22 SLT range (Figure 11). These calculated patterns give good qualitative agreement with the data presented. This model also predicts longitudinal variations in the ion drift. This has not yet been tested for in the AE-E data set. Such tests should provide a useful check on this proposed mechanism. The preliminary results presented here indicate that IDM data from the AE and the more recent Dynamics Explorer B spacecraft should continue to disclose some interesting and previously unobserved dynamical features of the low-latitude F-region.

REFERENCES

- Fejer, B. G., D. T. Farley, and C. A. Gonzales, F Region east-west drifts at Jicamarca, *J. Geophys. Res.*, *86*, 215, 1981
- Dachev, T. P. and J. C. G. Walker, Seasonal dependence of the distribution of large-scale plasma depletions in the low-latitude F-region, *J. Geophys. Res.*, *87*, 7625, 1982

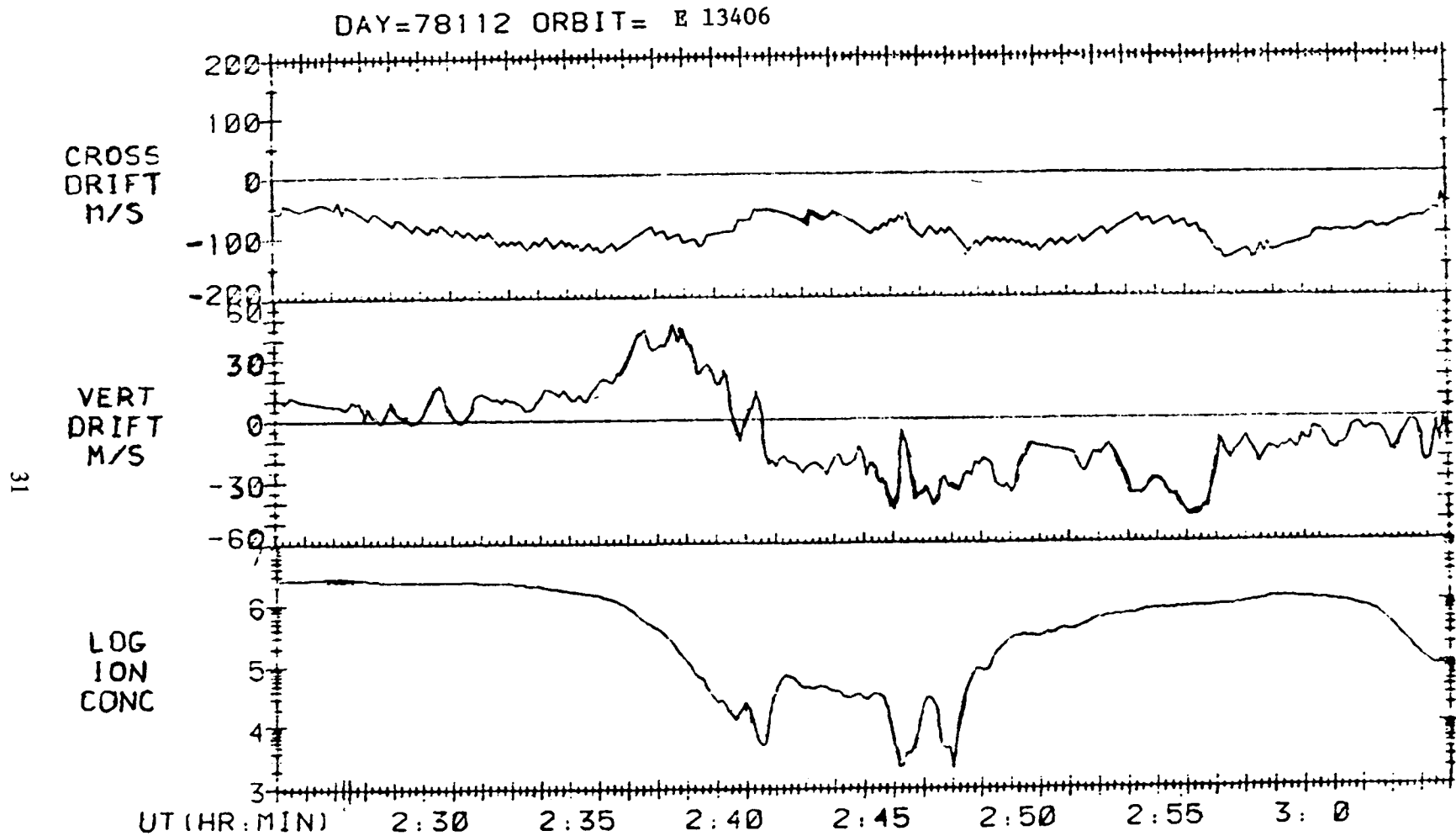


Figure 1. Data from AE-E orbit 13406 showing the sunset behavior of N_j and V_v at low dip latitudes at 315 km altitude in the Atlantic longitude sector on 22 April 1978. The post-sunset enhancement and reversal of V_y is clearly visible in this example of our routinely processed data.

END OF TAPE REACHED
INPUT 0 FOR AVERAGE PLOT
INPUT 1 FOR NEW TAPE
INPUT 2 FOR REPLOT
WITH FLYER REJECTION:

AE-E

78213 - 78273

ALT RANGE 200. 500.
LAT RANGE -90. 90.
LONG RANGE -180. 180.
ILAT RANGE 0. 90.
DLAT RANGE -20. 20.
VEL RANGE -125. 125.
MINIMUM NI 3000.

RUN NUMBER 213

32

VERTICAL
ION
VELOCITY
(M/S)

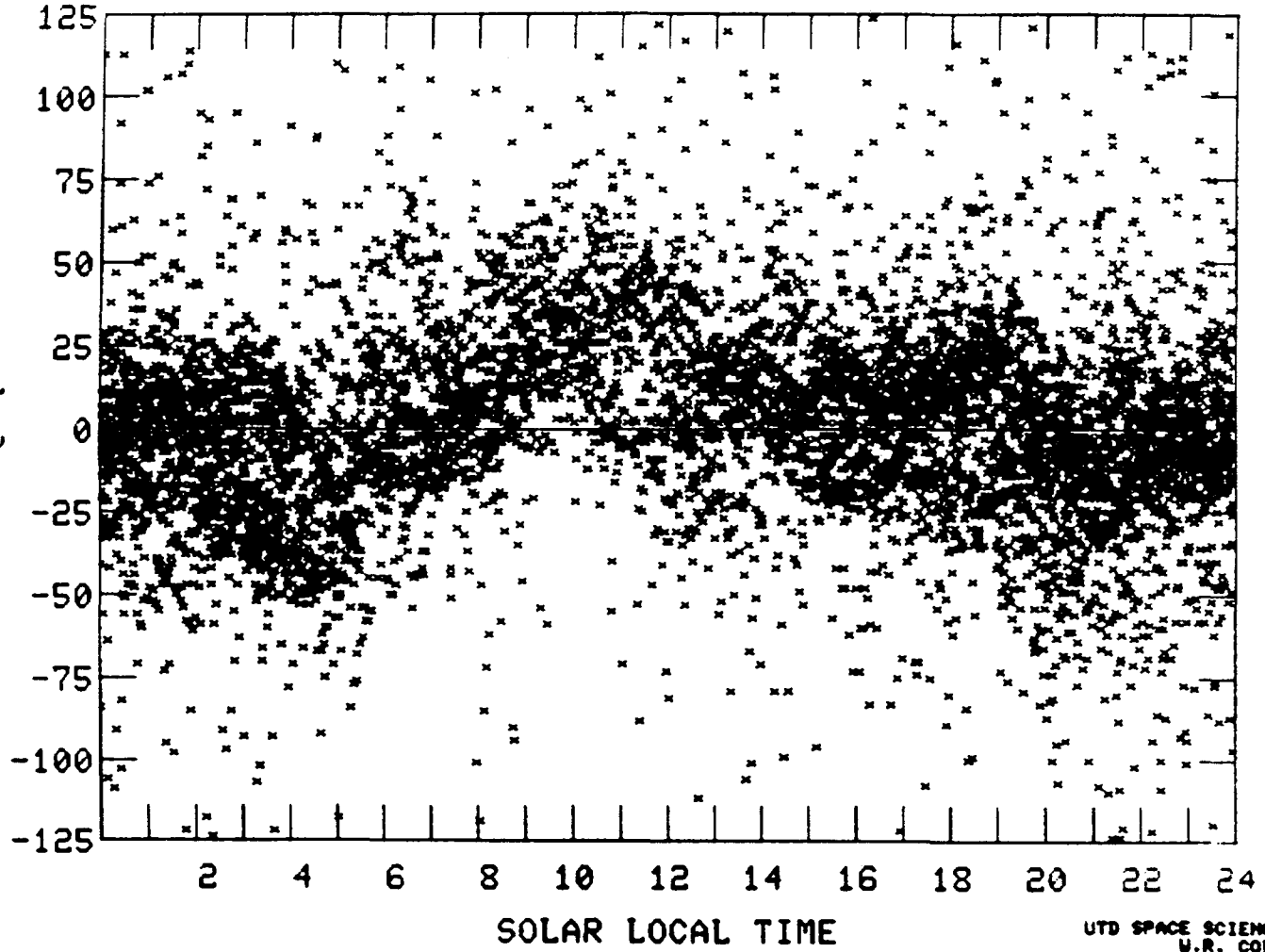


Figure 2a. Aug - Sept 1978
-20° to 20° DLAT

UTD SPACE SCIENCES
U.R. COLEY

HIT RETURN FOR
RUN STATISTICS

AE-E

78213 - 78273

ALT RANGE	200.	500.
LAT RANGE	-90.	90.
LONG RANGE	-180.	180.
ILAT RANGE	0.	90.
DLAT RANGE	-20.	20.
VEL RANGE	-125.	125.
MINIMUM NI		3000.

RUN NUMBER 813

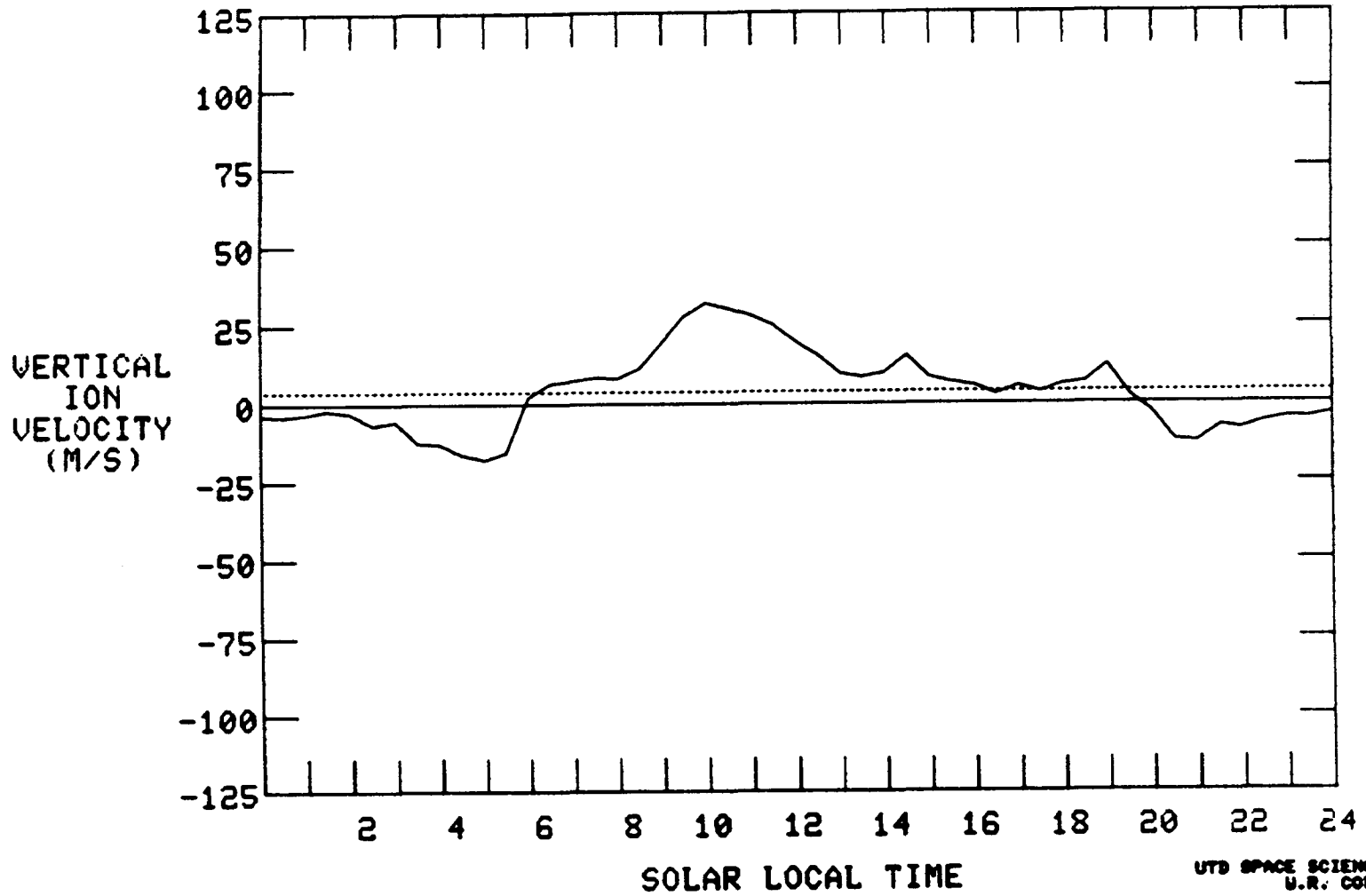


Figure 2b. Aug - Sept 1978 -20° to 20° DLAT

JICAMARCA VERTICAL DRIFT

JULY - AUG 1968-1971

34

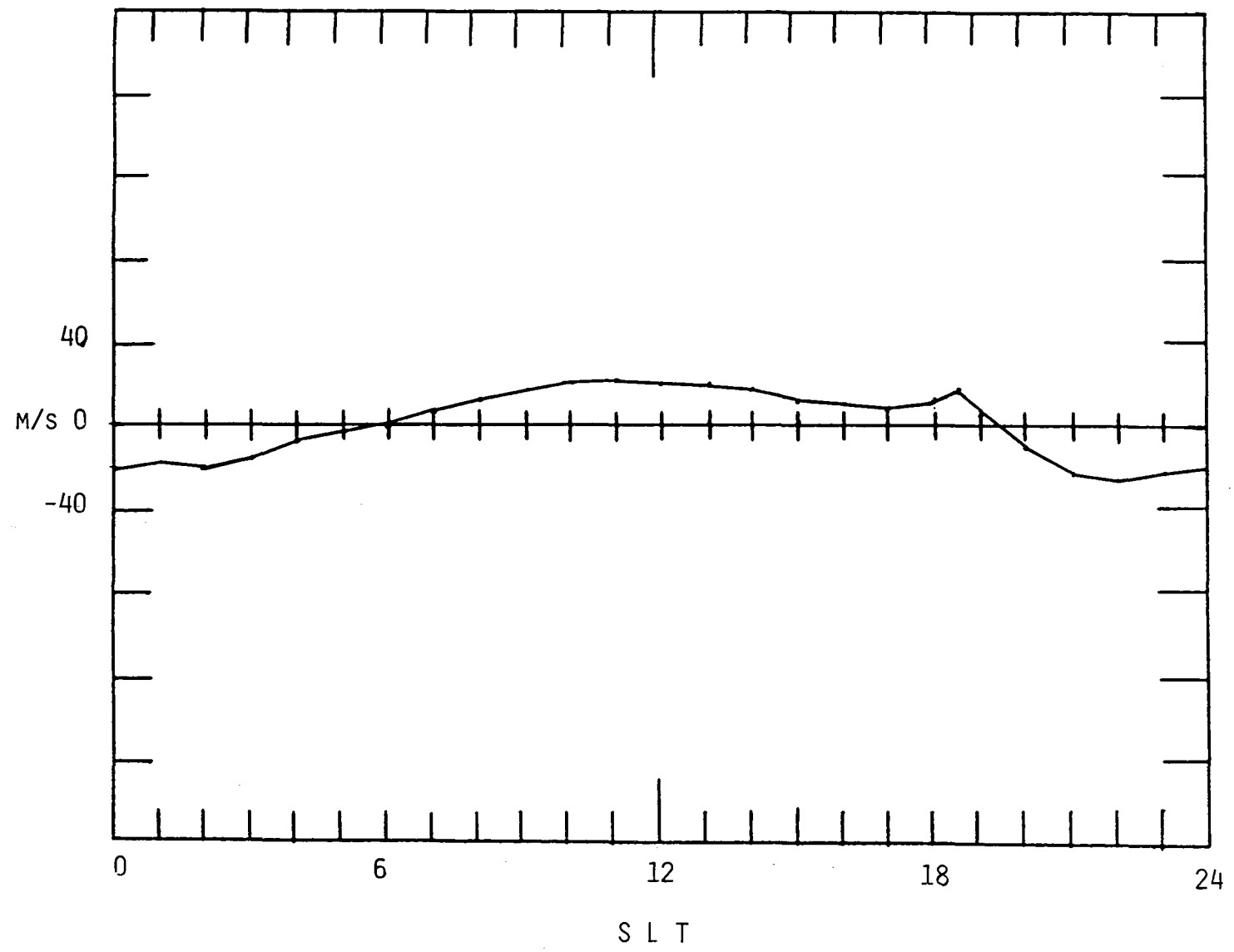


Figure 3

END OF TAPE REACHED
INPUT 0 FOR AVERAGE PLOT
INPUT 1 FOR NEW TAPE :

AE-E
79121 - 79212

ALT	RANGE	200.	500.
LAT	RANGE	-80.	90.
LONG	RANGE	-180.	180.
ILAT	RANGE	0.	90.
DLAT	RANGE	-20.	20.
UEL	RANGE	-100.	100.
MINIMUM NI			3000.

RUN NUMBER 139

35

VERTICAL
ION
VELOCITY
(M/S)

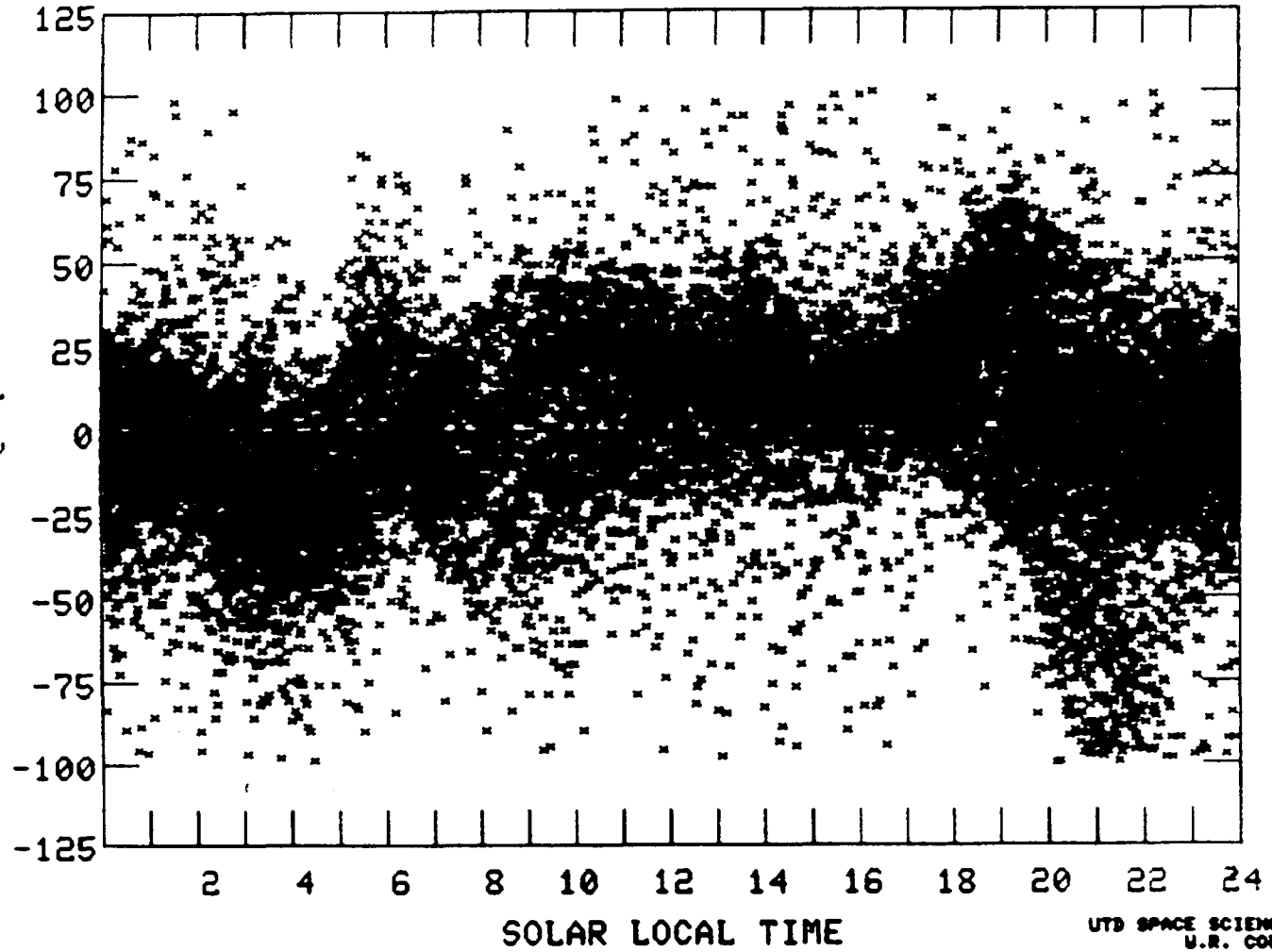


Figure 4a. May - July 1979 -20° to 20° DLAT

TT06A -- STOP 1

PDS>

AE-E

79121 - 79212

ALT RANGE	200.	500.
LAT RANGE	-90.	90.
LONG RANGE	-180.	180.
ILAT RANGE	0.	90.
DLAT RANGE	-20.	20.
VEL RANGE	-100.	100.
MINIMUM MI		3000.

RUN NUMBER 130

36

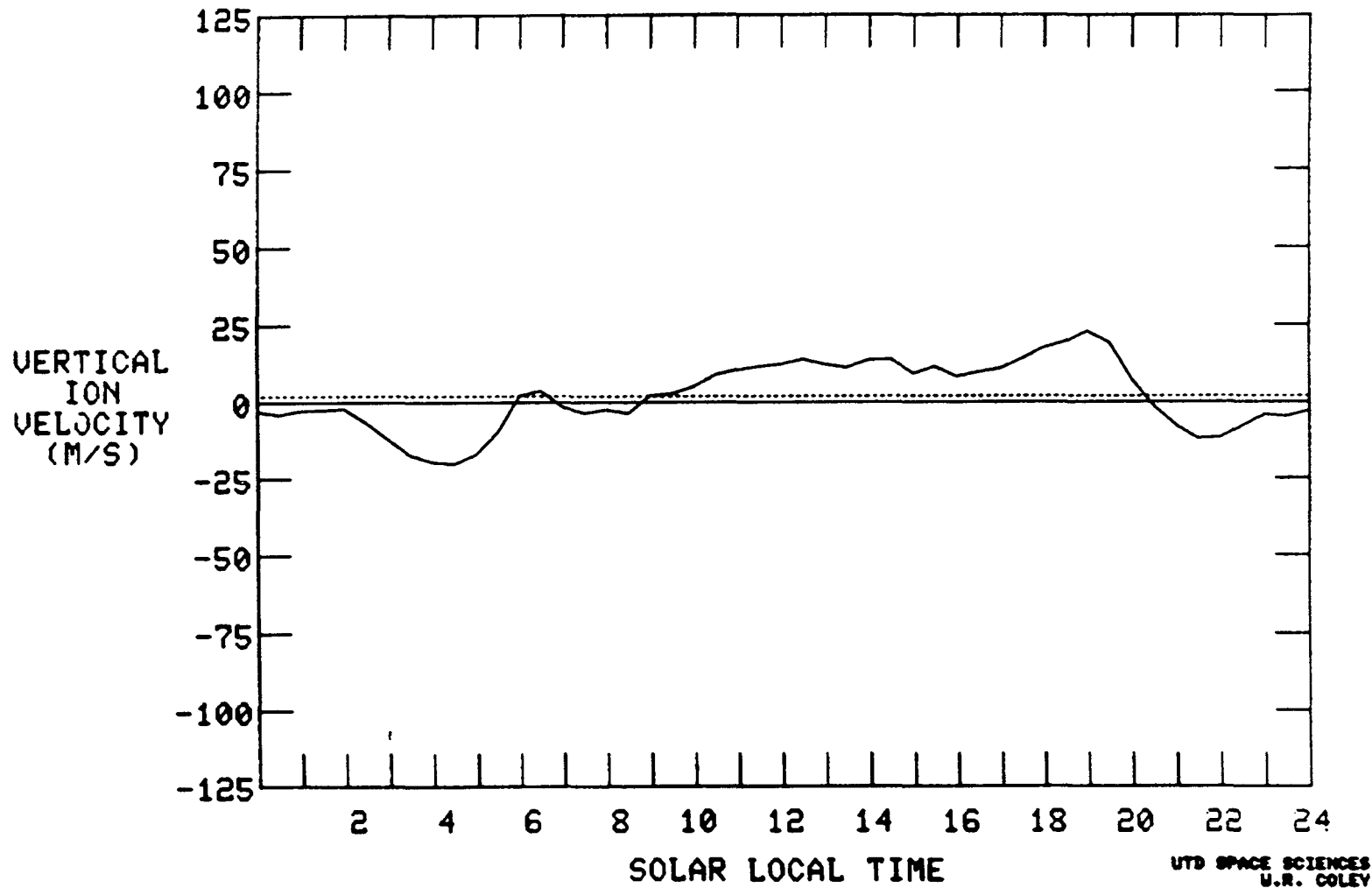


Figure 4b. May - July 1979 -20° to 20° DLAT

END OF TAPE REACHED
INPUT 0 FOR AVERAGE PLOT
INPUT 1 FOR NEW TAPE :

AE-E

79181 - 79212

ALT RANGE	200.	500.
LAT RANGE	-90.	90.
LONG RANGE	-180.	180.
ILAT RANGE	0.	90.
DLAT RANGE	10.	20.
VEL RANGE	-100.	100.
MINIMUM NI		3000.

RUN NUMBER 136

37

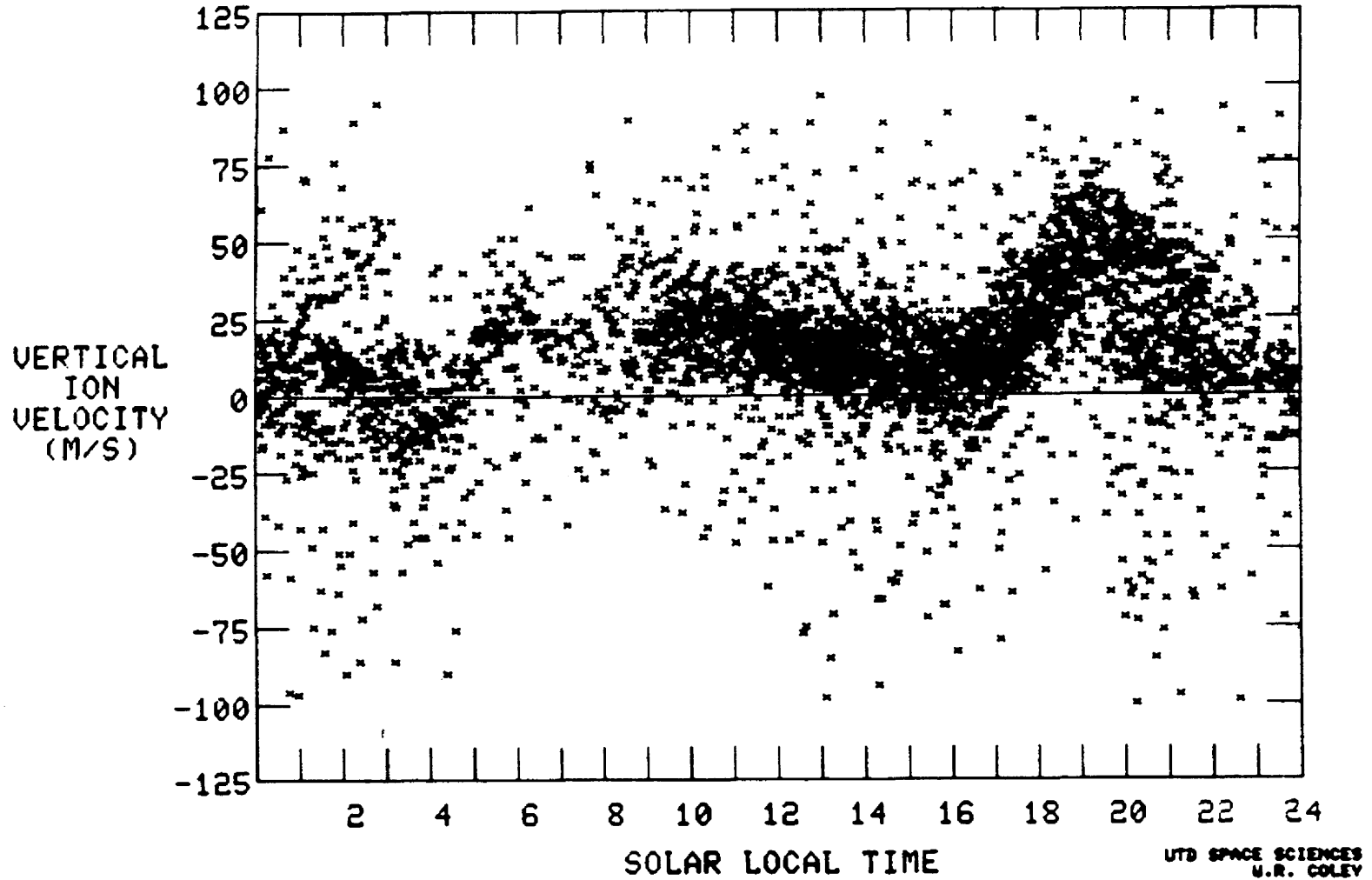


Figure 5a. May - July 1979 10° to 20° DLAT

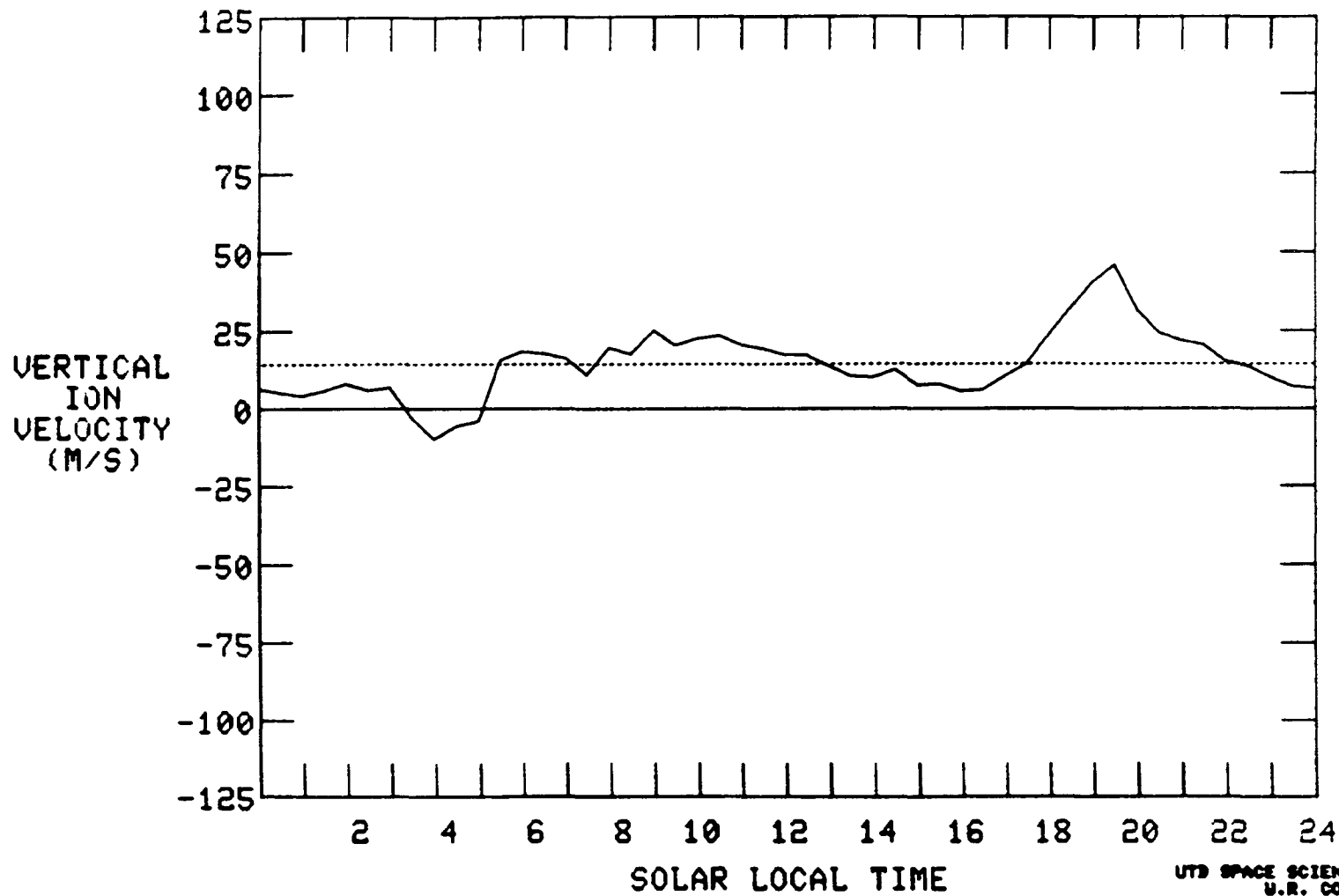
PT08A -- STOP 1

985>

AE-E
79121 - 79212

ALT RANGE	200.	500.
LAT RANGE	-50.	50.
LONG RANGE	-100.	100.
ILAT RANGE	0.	90.
DLAT RANGE	10.	20.
UEL RANGE	-100.	100.
MINIMUM MI		3000.

RUN NUMBER 136



38

Figure 5b. May - June 1979 10° to 20° DLAT

END OF TAPE REACHED
INPUT 0 FOR AVERAGE PLOT
INPUT 1 FOR NEW TAPE :

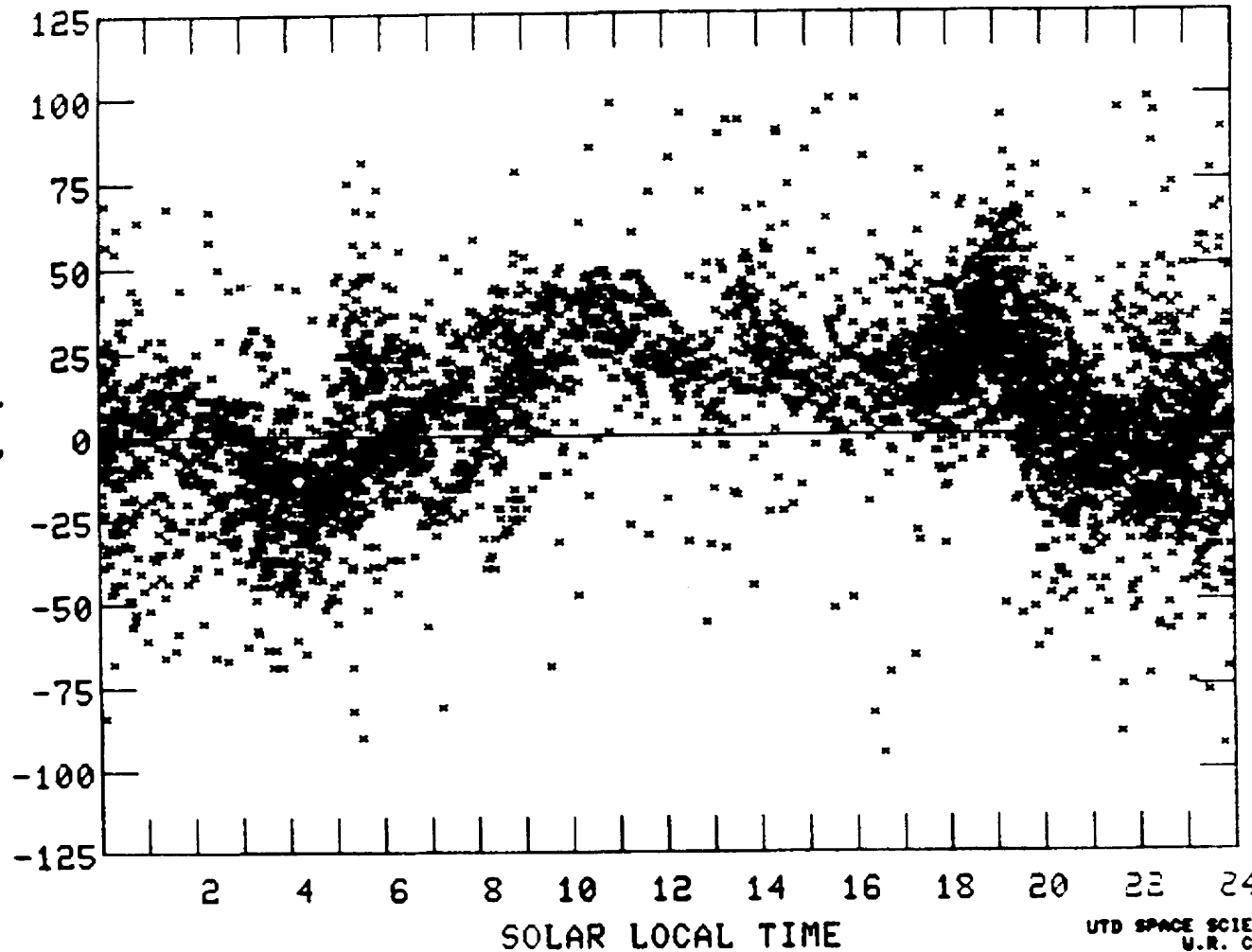
AE-E
79121 - 79212

ALT RANGE	200.	500.
LAT RANGE	-50.	50.
LONG RANGE	-180.	180.
ILAT RANGE	0.	90.
DLAT RANGE	0.	10.
UEL RANGE	-100.	100.
MINIMUM MI		3000.

RUN NUMBER 135

39

VERTICAL
ION
VELOCITY
(M/S)



UTD SPACE SCIENCES
U.R. COLEY

Figure 6a. May - July 1979 0° to 10° DLAT

TT06A -- STOP 1

PDS>

AE-E

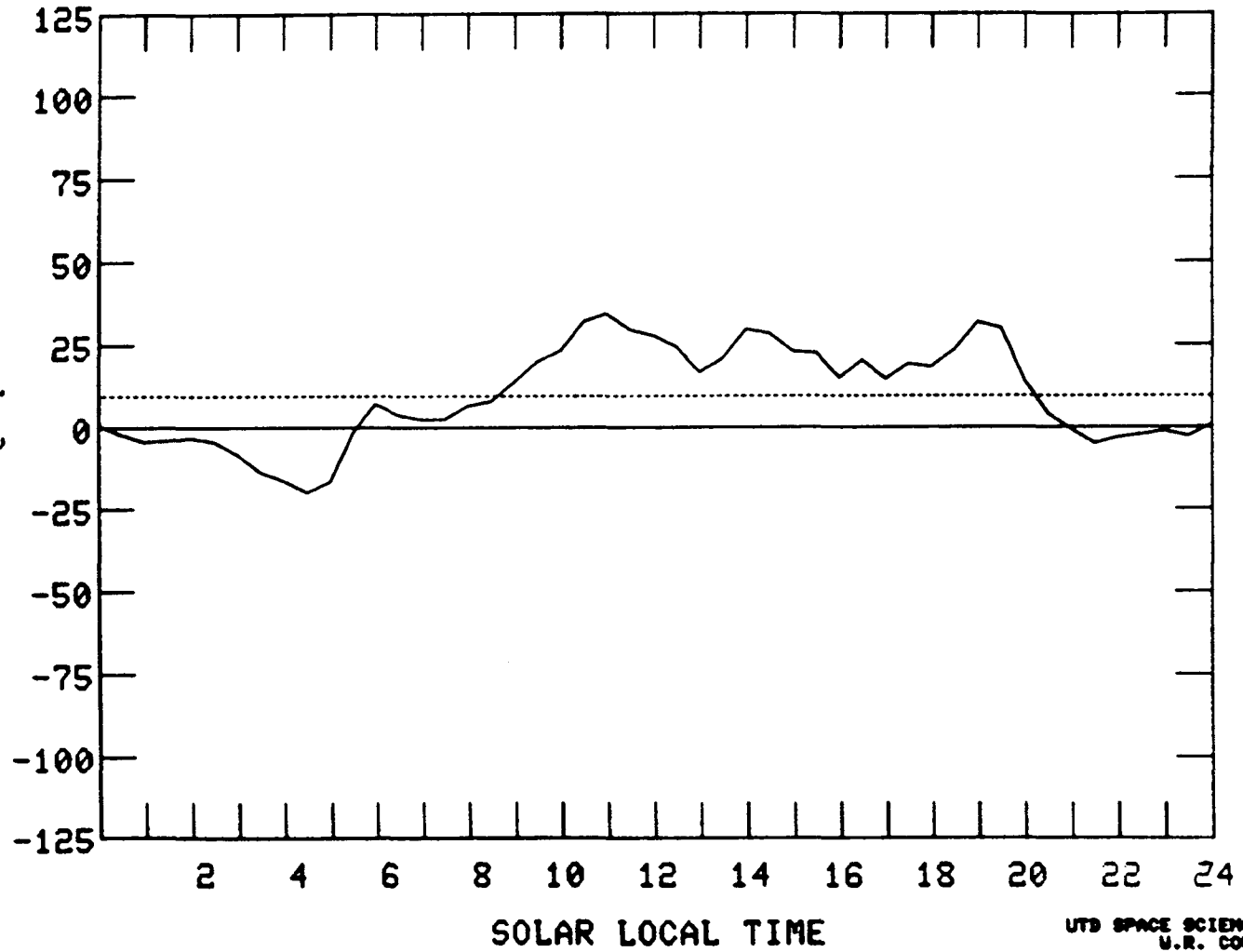
79121 - 79212

ALT RANGE	200.	500.
LAT RANGE	-90.	90.
LONG RANGE	-180.	180.
ILAT RANGE	0.	90.
DLAT RANGE	0.	10.
UEL RANGE	-100.	100.
MINIMUM NI		3000.

RUN NUMBER 135

40

VERTICAL
ION
VELOCITY
(M/S)



UTS SPACE SCIENCES
U.R. COLEY

Figure 6b. May - July 1979 0° to 10° DLAT

END OF TAPE REACHED
INPUT 0 FOR AVERAGE PLOT
INPUT 1 FOR NEW TAPE :

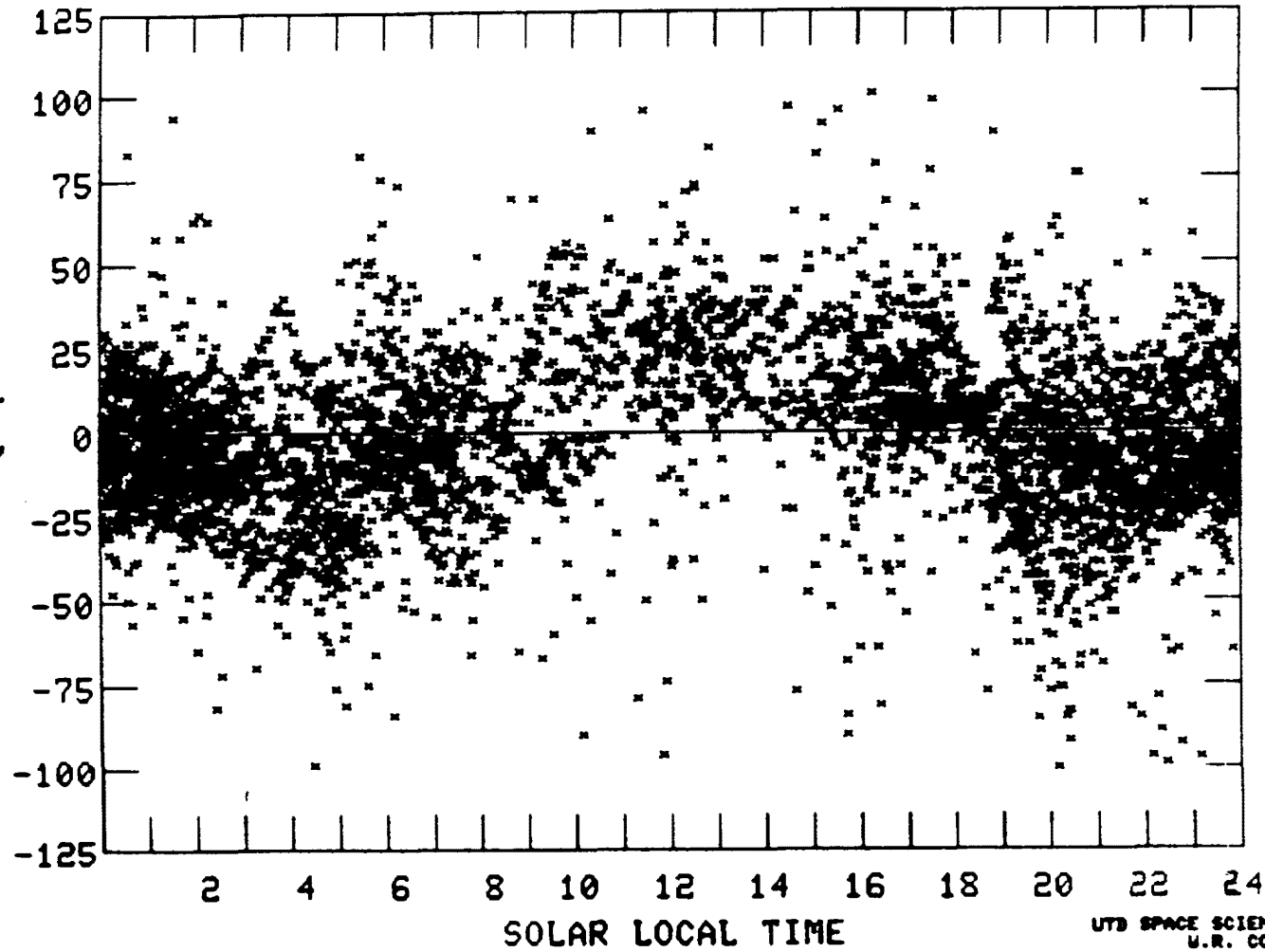
AE-E
79121 - 79212

ALT RANGE 200. 500.
LAT RANGE -90. 90.
LONG RANGE -180. 180.
ILAT RANGE 0. 90.
DLAT RANGE -10. 0.
VEL RANGE -100. 100.
MINIMUM NI 3000.

RUN NUMBER 137

41

VERTICAL
ION
VELOCITY
(M/S)



UTS SPACE SCIENCES
U.R. COLEY

Figure 7a. May - July 1979 -10° to 0° DLAT

TT08A -- STOP 1

P880

AE-E

79181 - 79212

ALT RANGE	800.	500.
LAT RANGE	-90.	90.
LONG RANGE	-100.	100.
ILAT RANGE	0.	90.
DLAT RANGE	-10.	0.
VEL RANGE	-100.	100.
MINIMUM NI		3000.

RUN NUMBER 137

42

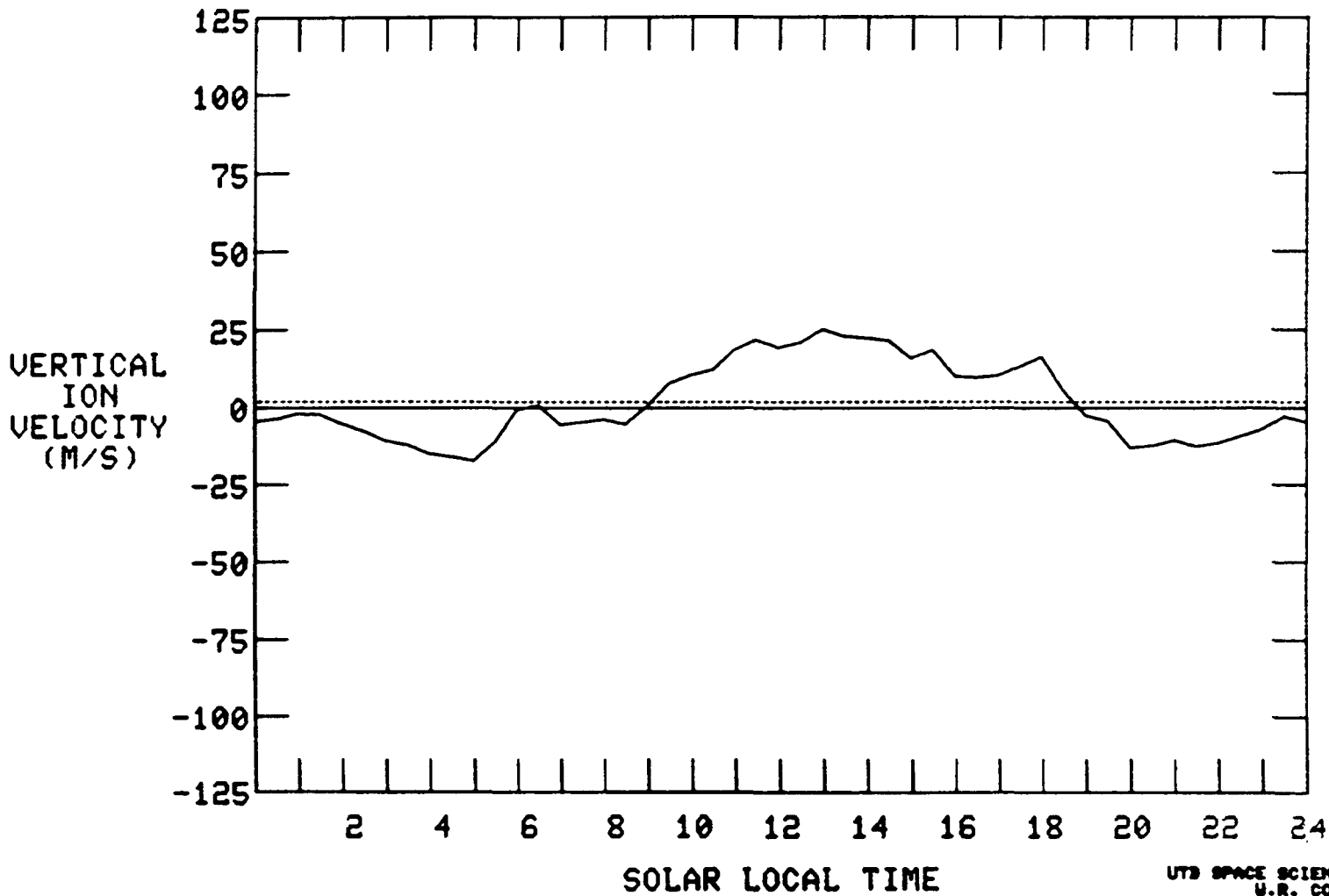


Figure 7b. May - July 1979 -10° to 0° DLAT

END OF TAPE REACHED
INPUT 0 FOR AVERAGE PLOT
INPUT 1 FOR NEW TAPE :

AE-E

79121 - 79212

ALT RANGE	200.	500.
LAT RANGE	-90.	90.
LONG RANGE	-180.	180.
ILAT RANGE	0.	90.
DLAT RANGE	-20.	-10.
UEL RANGE	-100.	100.
MINIMUM NI		3000.

RUN NUMBER 138

43

VERTICAL
ION
VELOCITY
(M/S)

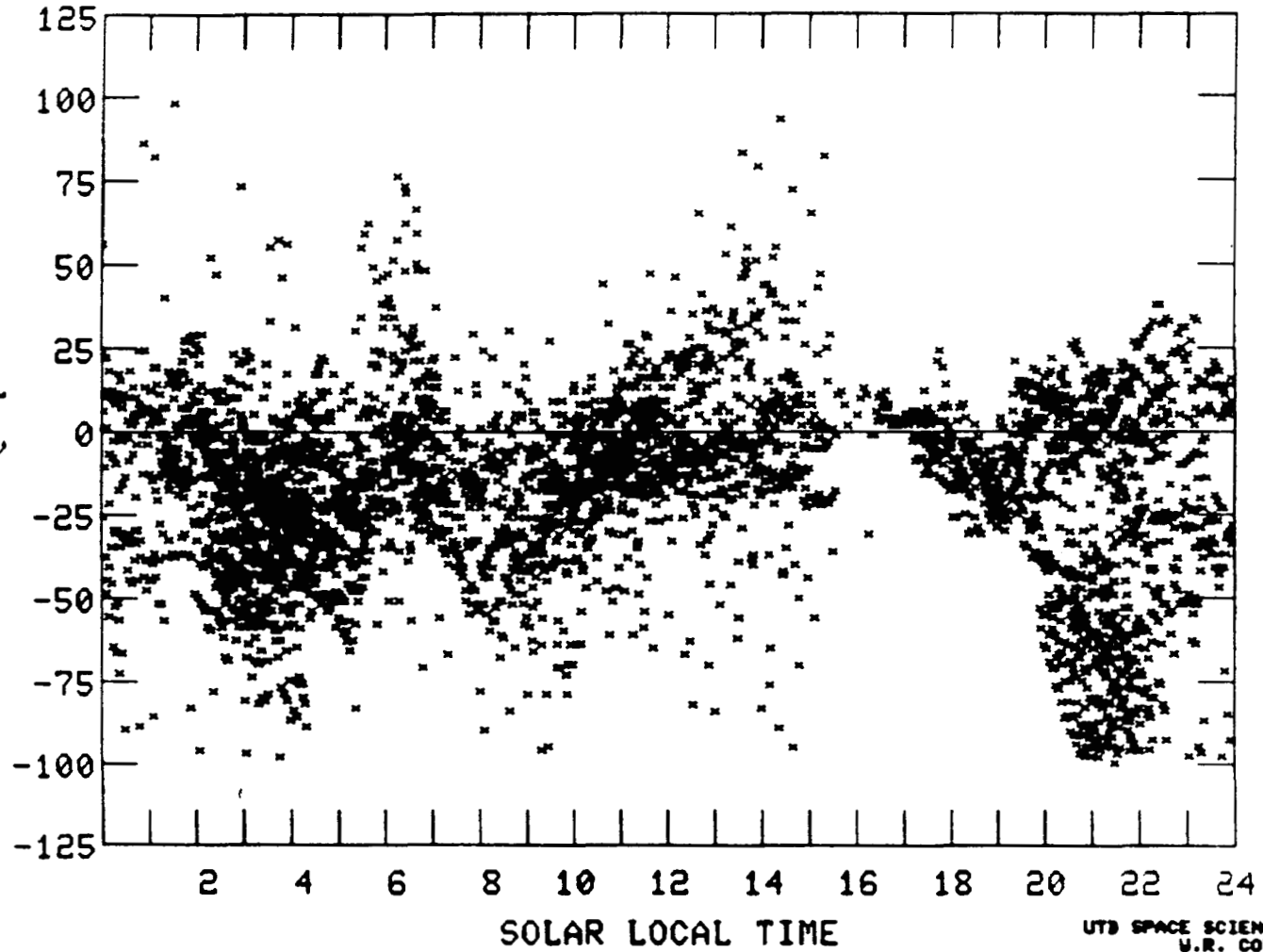


Figure 8a. May - July 1979 -20° to 10° DLAT

UTB SPACE SCIENCES
U.R. COLEY

TT08A -- STOP 1

PBS>

AE-E

78121 - 78812

ALT RANGE	800.	800.
LAT RANGE	-90.	90.
LONG RANGE	-180.	180.
ILAT RANGE	0.	90.
DLAT RANGE	-30.	-10.
VEL RANGE	-100.	100.
MINIMUM NZ		3000.

RUN NUMBER 138

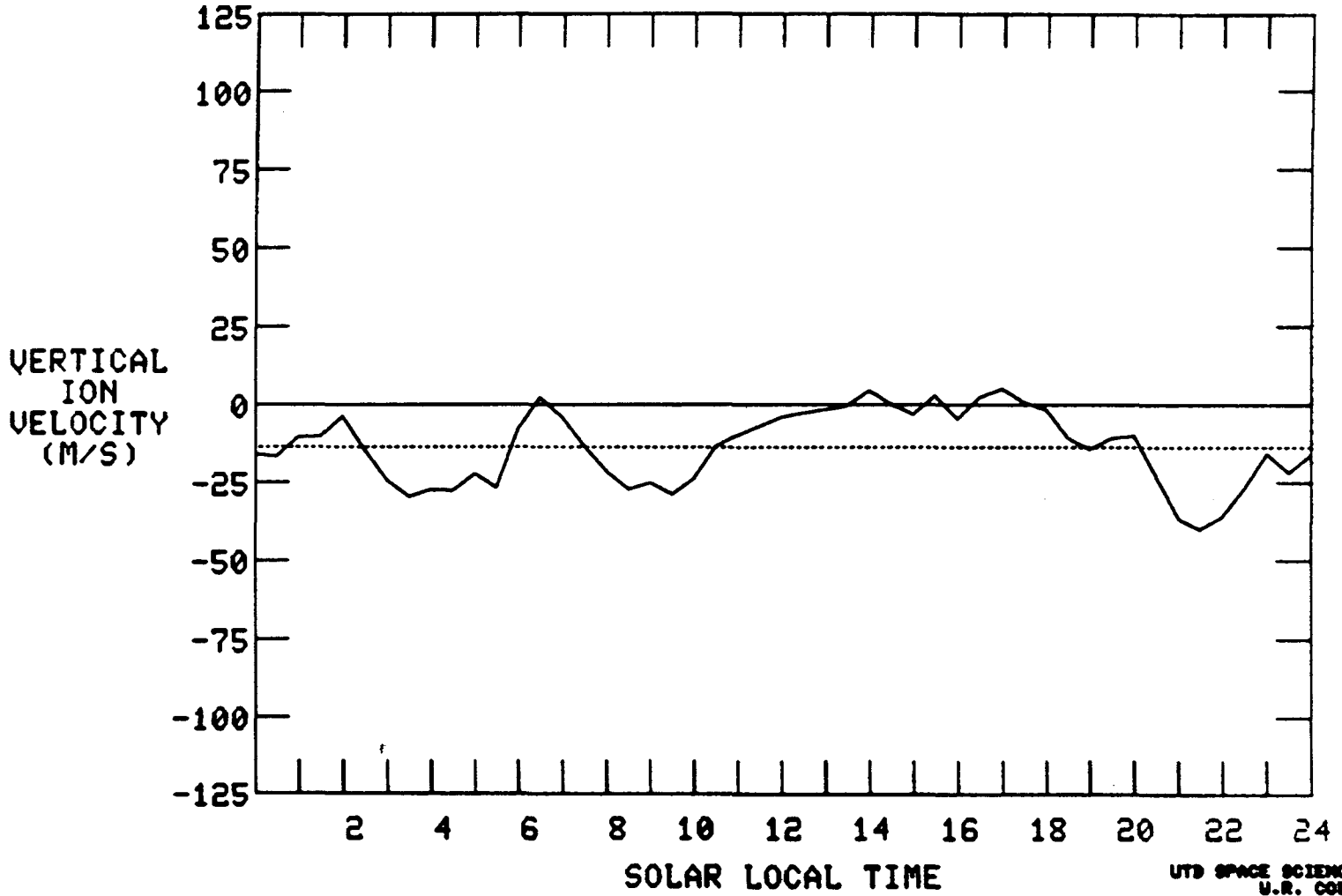


Figure 8b. May - July 1979 -20° to -10° DLAT

END OF TAPE REACHED
INPUT 0 FOR AVERAGE PLOT
INPUT 1 FOR NEW TAPE :

AE-E

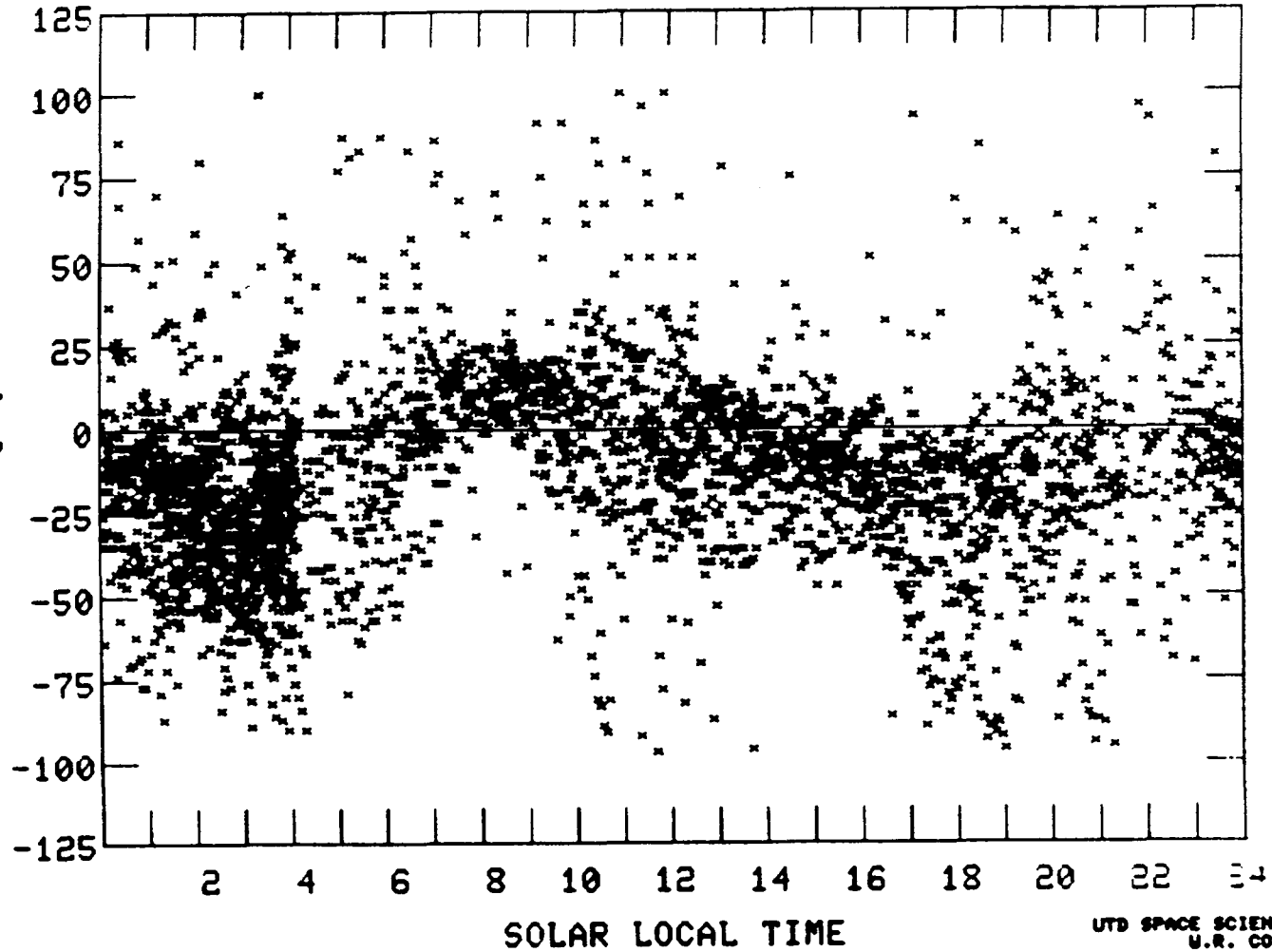
77305 - 78031

ALT RANGE	200.	500.
LAT RANGE	-90.	90.
LONG RANGE	-180.	180.
ILAT RANGE	0.	90.
DLAT RANGE	10.	20.
VEL RANGE	-100.	100.
MINIMUM MI		3000.

RUN NUMBER 186

45

VERTICAL
ION
VELOCITY
(M/S)



UTD SPACE SCIENCES
U.R. COLEY

Figure 9a. Nov 1977 - Jan 1978
10° to 20° DLAT

TT14A -- STOP 1

PDS>

AE-E
77306 - 78031

ALT RANGE	200.	500.
LAT RANGE	-90.	90.
LONG RANGE	-180.	180.
ILAT RANGE	0.	90.
DLAT RANGE	10.	20.
VEL RANGE	-100.	100.
MINIMUM NI		3000.

RUN NUMBER 186

46

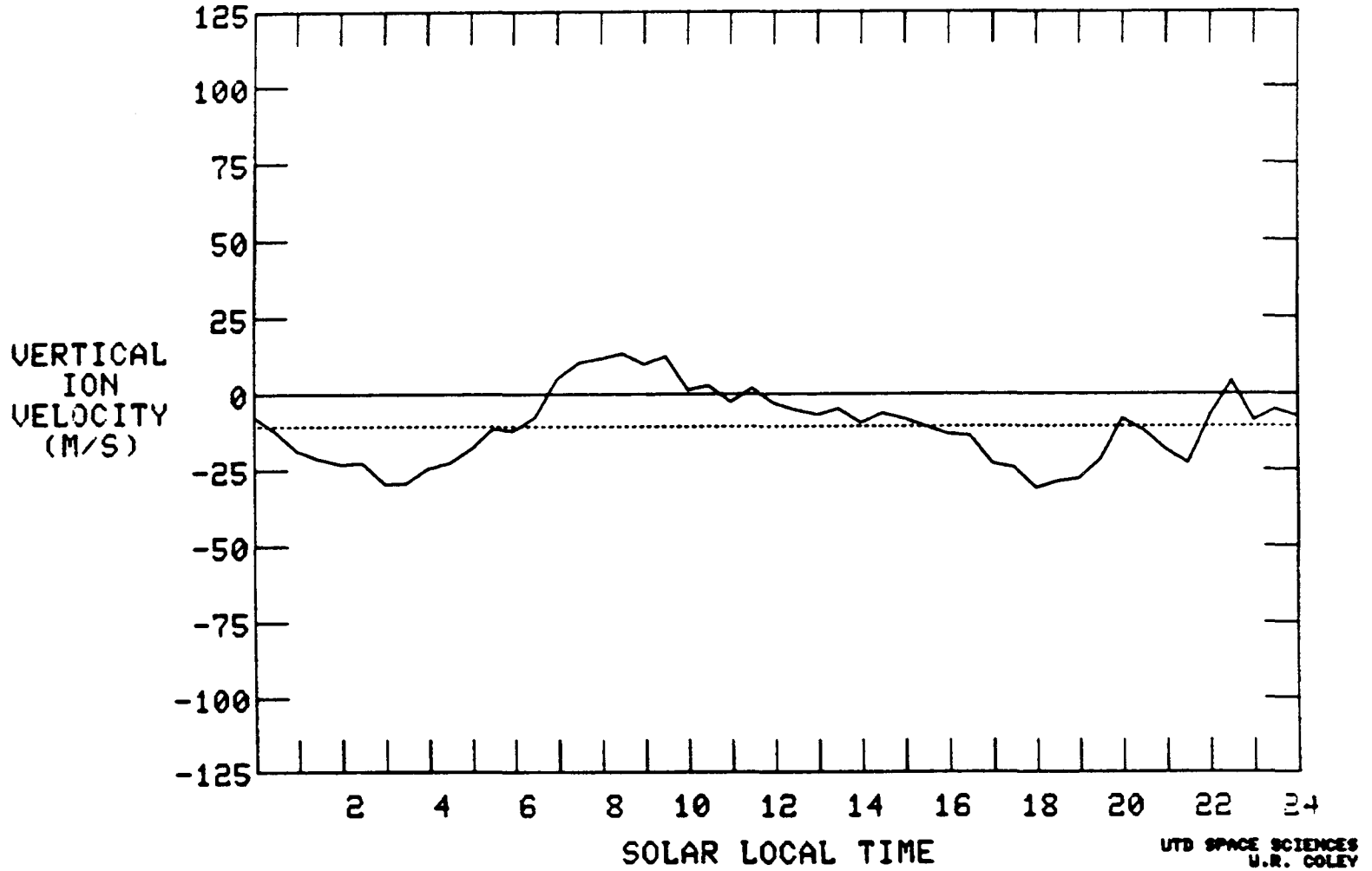


Figure 9b. Nov 1977 - Jan 1978 10° to 20° DLAT

END OF TAPE REACHED
INPUT 0 FOR AVERAGE PLOT
INPUT 1 FOR NEW TAPE :

AE-E
77306 - 78031

ALT RANGE	200.	500.
LAT RANGE	-90.	90.
LONG RANGE	-180.	180.
ILAT RANGE	0.	50.
DLAT RANGE	-20.	-10.
VEL RANGE	-100.	100.
MINIMUM NI		3000.

RUN NUMBER 182

VERTICAL
ION
VELOCITY
(M/S)

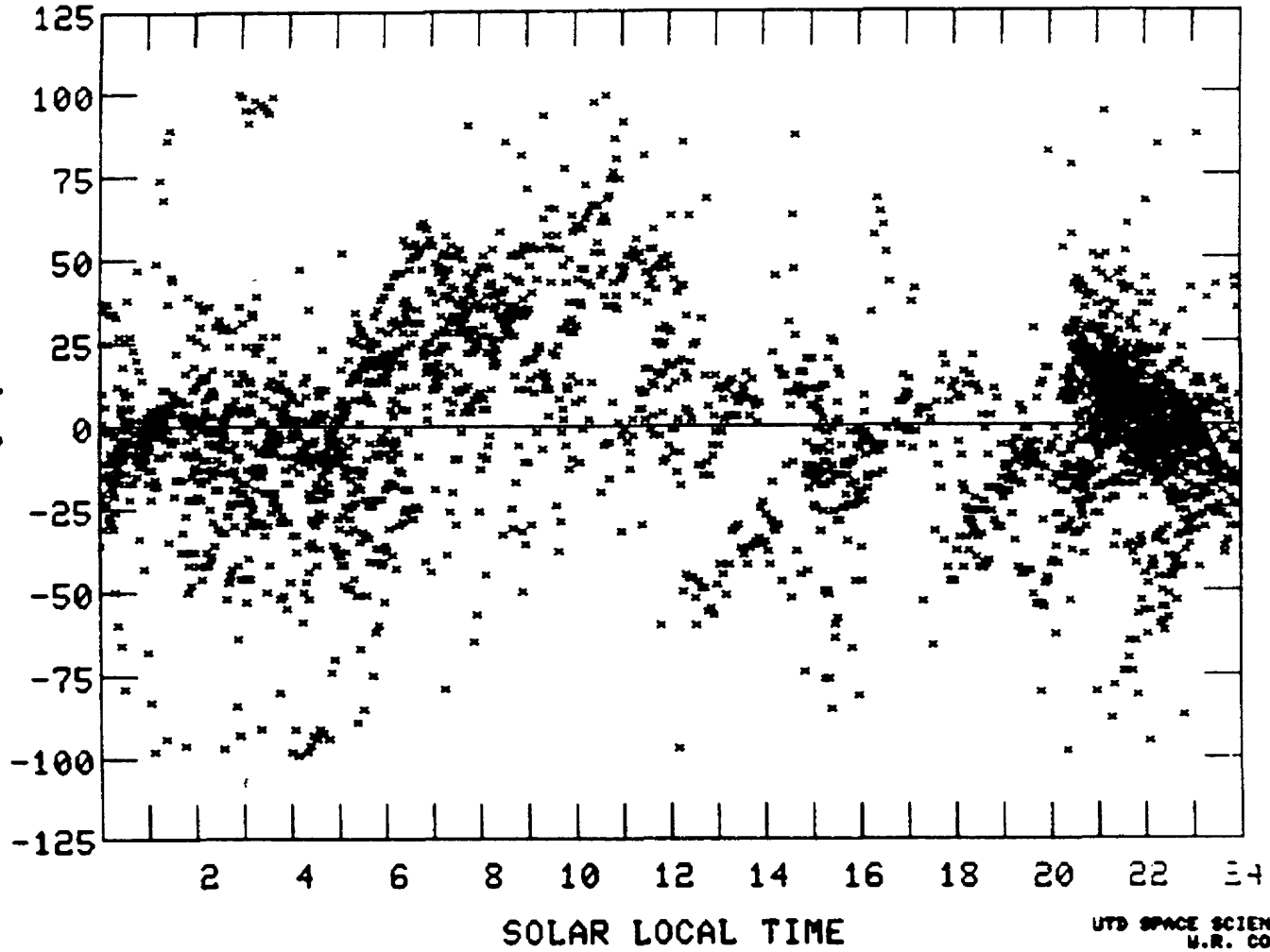


Figure 10a. Nov 1977 - Jan 1978
-20° to -10° DLAT

TT140 -- STOP 1

PDS>

AE-E

77305 - 78031

ALT RANGE	200.	500.
LAT RANGE	-50.	90.
LONG RANGE	-180.	180.
ILAT RANGE	0.	90.
DLAT RANGE	-20.	-10.
VEL RANGE	-100.	100.
MINIMUM NI		3000.

RUN NUMBER 182

48

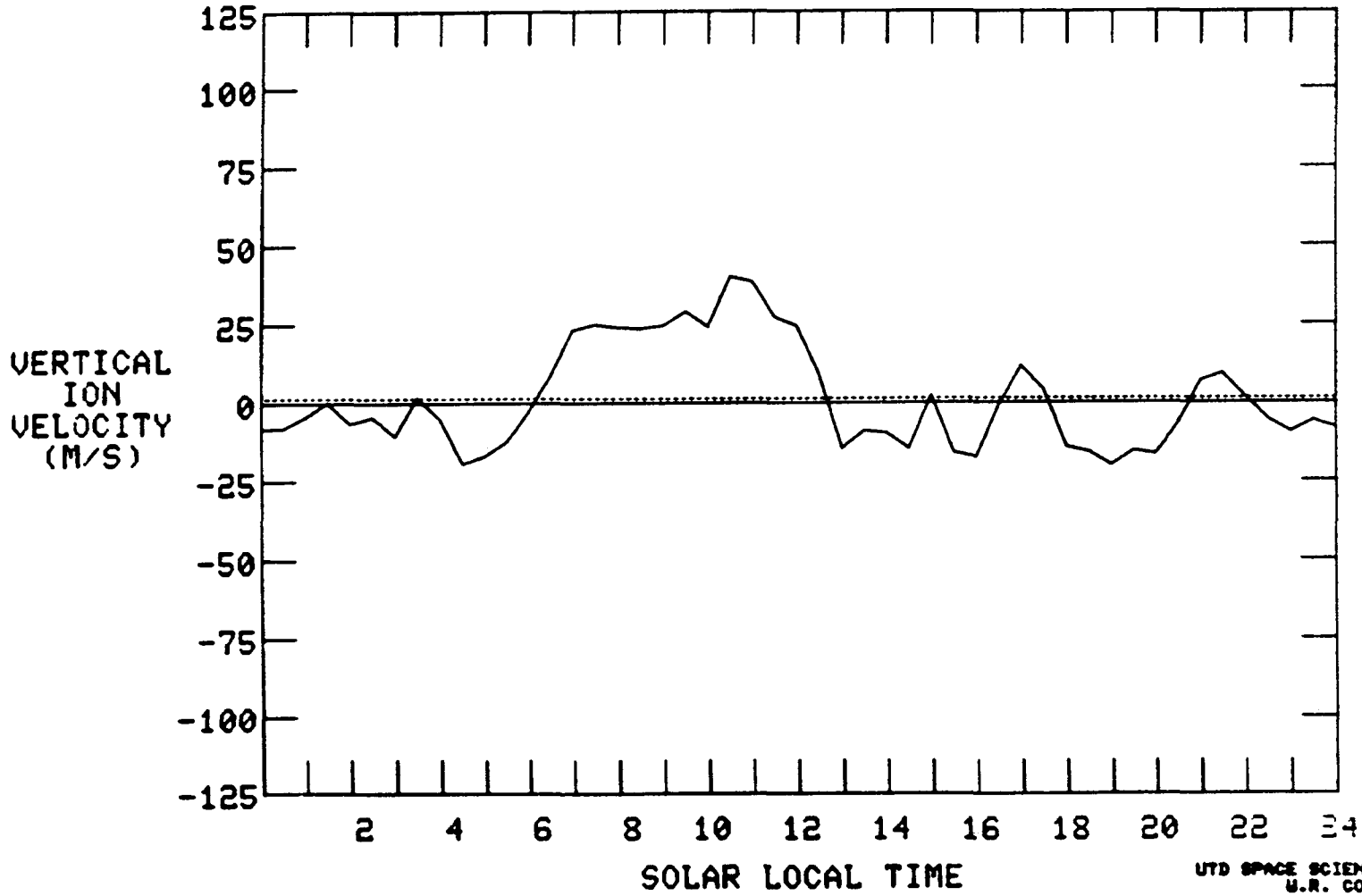


Figure 10b. Nov 1977 - Jan 1978 -20° to -10° DLAT

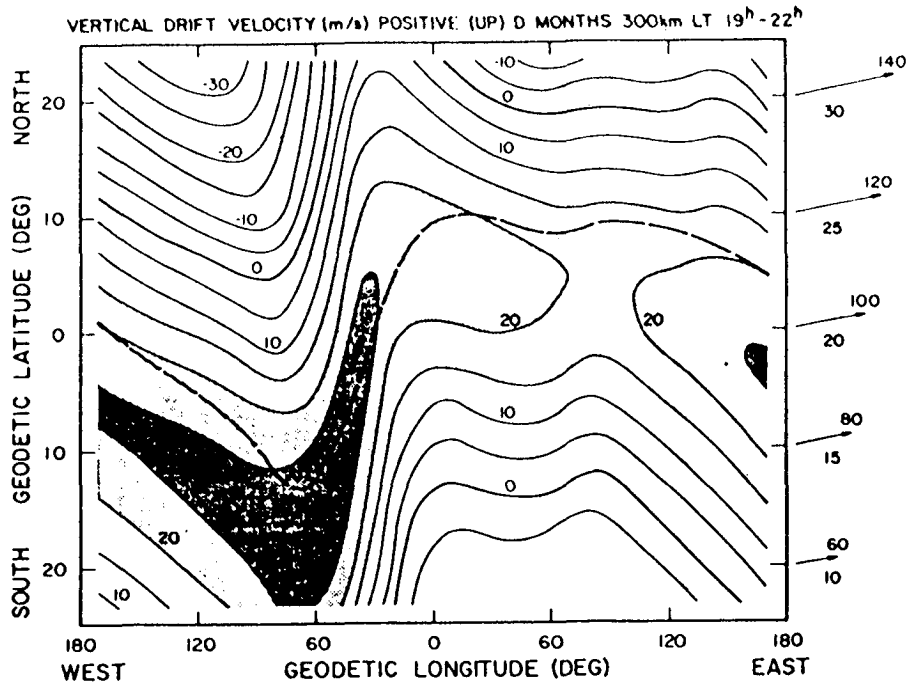


Figure 11. Contours of vertical ion drift velocity calculated for D months (northern hemisphere winter). A realistic model of the magnetic field at 300-km altitude is used for magnitude, inclination, and declination. The electric field is assumed to be constant and eastward at a value of 0.6 mV m^{-1} . The wind field varies linearly with geodetic latitude as indicated on the right-hand side of the figure. The dashed line denotes the geomagnetic equator, and the letter J refers to the Jicamarca Observatory. Regions of maximum upward drift velocity are shaded. Their locations correspond to the distribution of depleted plasma regions observed at winter solstice and shown in Figure 6.

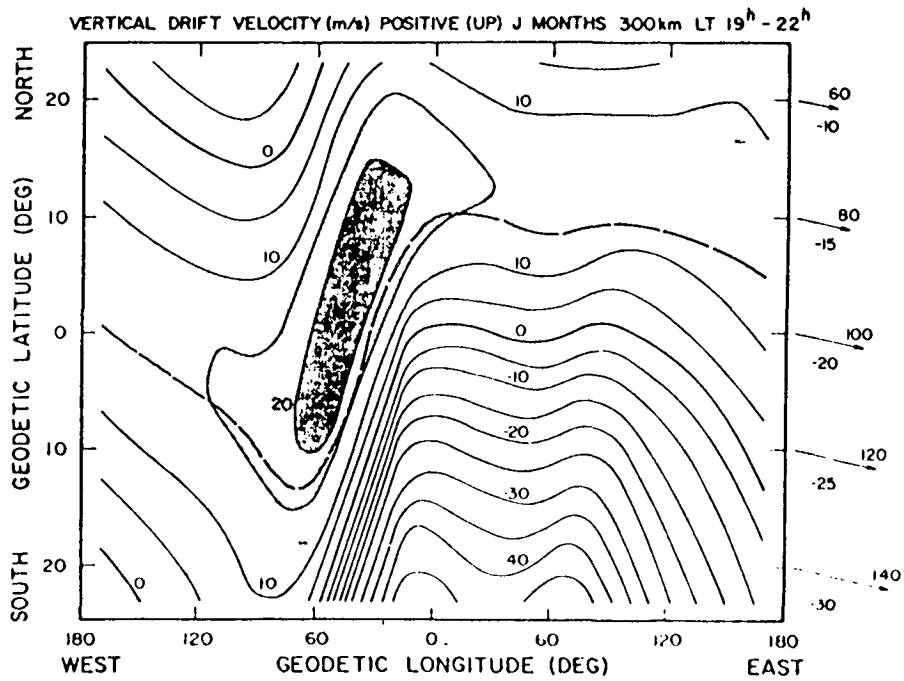


Figure 12. Vertical ion drift velocity calculated for northern hemisphere summer (J months). The wind field is the same as that used in Figure 11, with appropriate seasonal changes. Regions of maximum upward drift are shaded; their distribution corresponds closely to the observations of depleted plasma regions shown in Figure 7.